

Kinetics of stimulated polariton scattering in planar GaAs microcavities resonantly excited with a linearly polarized light

A. A. Demenev,¹ S. S. Gavrilov,^{1,2} and V. D. Kulakovskii¹¹*Institute of Solid State Physics, RAS, Chernogolovka 142432, Russia*²*A.M. Prokhorov General Physics Institute, RAS, Moscow 119991, Russia*

(Received 18 September 2009; revised manuscript received 23 December 2009; published 20 January 2010)

Nonequilibrium transitions in the cavity polariton system are investigated under nanosecond-long pulsed excitation with linearly polarized light (TE or TM modes) near the magic angle. The main objective is to clarify the influence of the polarization-dependent properties of the polariton-polariton interaction on (i) instabilities in a driven lower polariton mode and (ii) the temporal hysteresis effects in the kinetics of the scattered polariton population. The driven mode retains the polarization of the exciting pulse and exhibits instabilities typical of the scalar (“spinless”) polariton system excited with circularly polarized light. No increase in the instability threshold for the driven mode and, as a consequence, no polarization multistability discussed for the spinor polariton system [N. A. Gippius *et al.*, Phys. Rev. Lett. **98**, 236401 (2007)] is observed. Polarization of the scattering signal at the zero wave vector and that of the driven mode are mutually perpendicular, due to the polarization dependence of the exciton-exciton interaction. At the same time, at pump intensities well above the threshold of stimulated scattering, the signal exhibits a markable decrease (up to 25%) of the polarization degree during the pulse transmission.

DOI: [10.1103/PhysRevB.81.035328](https://doi.org/10.1103/PhysRevB.81.035328)

PACS number(s): 71.36.+c, 42.65.Pc, 42.55.Sa

I. INTRODUCTION

Microcavity (MC) exciton polaritons are elementary bosonlike excitations with an extremely small effective mass on the order of 10^{-5} of the free-electron mass and a specific dispersion with an inflection point at small wave vectors ($|\mathbf{k}| \sim 10^4 \text{ cm}^{-1}$).^{1–3} These peculiarities result in a variety of interesting effects in a dense polariton system. Parametric polariton-polariton scattering and Bose-Einstein condensation are two of the most striking features in the photoexcited system of cavity polaritons.^{4–13}

Stimulated scattering appears in planar MCs under excitation slightly above the lower polariton (LP) branch and has the minimum threshold for excitation close to the inflection point in the dispersion curve.^{4,5,9} The unusual behavior of stimulated scattering [that exhibits a predominant population of $\mathbf{k}=0$ and $\mathbf{k}=2\mathbf{k}_p$ modes almost regardless of pump energy and quasimomentum \mathbf{k}_p (Refs. 8 and 9)] was shown to be coming from the interplay between two distinct instabilities each induced by the polariton-polariton repulsive interaction. They are the single-mode instability (bistability) of the driven mode with respect to the incident pump^{14–20} and the parametric instability of the driven system with respect to the intermode polariton-polariton scattering.^{21–23} The unusually low threshold of the stimulated scattering under the excitation near the inflection point comes from the simultaneous fulfillment of both the energy and momentum conservation laws.

An important peculiarity of cavity polaritons is related to their polarization, or pseudospin, degree of freedom. Two possible spin projections onto the normal to the MC plane correspond to the right (σ^+) and left (σ^-) circular polarizations of counterpart photons. These two components are mixed for nonzero in-plane wave vectors (\mathbf{k}) because of the splitting of polariton modes into the TE and TM states with mutually perpendicular linear polarizations,²⁴ which comes

from the polarization dependence of field penetration in a dielectric mirror. The spin-dependent polariton coupling leads to markable collective effects in the system of interacting polaritons.^{25–28}

The stimulated scattering under excitation with circularly polarized light near the magic angle shows a negligible depolarization effect in the scattered modes.^{29,30} It enables us to consider the system of circularly polarized polaritons as a spinless (“scalar”) one. Within this approximation, complicated hysteresis loops in the population kinetics of pumped and scattered LPs under a nanosecond-long resonant excitation are explained qualitatively within the framework of the semiclassical model based on the Gross-Pitaevskii equations.^{31,32}

In contrast, no polarization conservation is observed in the stimulated scattering under the excitation with linearly or elliptically polarized light.^{5,25,27,30} The intermode scattering of two linearly polarized LPs results in the change in their polarization direction to the perpendicular one.²⁶ The inversion of the polarization is due to the different signs of the polariton-polariton interaction constants for LPs with the same and opposite spin orientations: the attraction between polaritons with opposite spins corresponds to the negative sign of the matrix element of the polariton-polariton interaction, α_2 , whereas the repulsion of polaritons with the same spin corresponds to the positive matrix element α_1 .^{33,34}

The relation between the values of the LP interaction coefficients, α_1 and α_2 , strongly depends on the properties of the MC structure. At present it is generally accepted that for a typical GaAs microcavity $|\alpha_2| \ll |\alpha_1|$, i.e., in a variety of pump conditions the attraction between excitons with opposite spins is much smaller than the exchange-induced repulsion between excitons in the same quantum state.³⁵ Theoretically, in the Hartree-Fock approximation for the system of 1s excitons the former should be completely absent ($\alpha_2=0$) (Refs. 33 and 36) and only the relatively weaker high-order

excitations give a nonzero contribution to α_2 .³³ The results of the recent experiments on the spin quantum beats in the GaAs cavity polariton system established that the relation $|\alpha_2/\alpha_1|$ is less than 10^{-1} .²⁶ In turn, this result led to the certain predictions concerning the polarization properties of the LP system response to external pumping, namely, the multistability of the driven LP mode under the conditions of resonant continuous-wave excitation.³⁷ According to Ref. 37, under the linear pumping the driven intracavity state may either be polarized linearly or acquire a high degree of circular (left or right) polarization. On the other hand, the threshold of stimulated LP scattering should be strongly dependent on pump polarization. In the limiting case $\alpha_2=0$, the threshold for linearly polarized excitation should be approximately two times larger than the threshold for circular excitation.

Nonconservation of polarization in LP-LP scattering excited with linearly or elliptically polarized light was observed in cw experiments.^{5,27} In the present work we examine the polarization properties of the driven mode and the polarization dependence of the threshold excitation magnitude under the pulsed excitation with nanosecond-long pulses near the inflection point of LP dispersion. We study the kinetics of both the driven LP mode and the signal of stimulated scattering under linearly polarized excitation. The main objective is to investigate how the kinetics of the driven and scattered modes in the spinor LP system is influenced by the above-mentioned instabilities (typical for the scalar LP system³¹) in conjunction with the polarization dependence of the LP-LP interactions. A strong effect is observed for the scattered mode at $\mathbf{k}=0$ that acquires inverted linear polarization near the threshold of the stimulated scattering and then shows a weak depolarization with time. However, (i) the threshold excitation densities are found to be almost coincident for circular and linear pump polarizations (no increase in the threshold is observed when the pump polarization was changed from circular to linear one) and, accordingly, (ii) no polarization multistability predicted in Ref. 37 is observed in the LP system driven with linearly polarized light.

The paper is organized as follows. In Sec. II, the sample structure and experimental setup are described. Time evolution of the intensity and spectral position of the driven LP mode is described in Sec. III; the experimental results are compared with the available theoretical predictions. Section IV is concerned with the polarization effects in the kinetics of stimulated LP-LP scattering.

II. EXPERIMENTAL

The MC structure grown by the metalorganic vapor-phase epitaxy technique has top (bottom) Bragg reflectors composed of 17 (20) $\lambda/4$ $\text{Al}_{0.13}\text{Ga}_{0.87}\text{As}/\text{AlAs}$ layers. The $3\lambda/2$ GaAs cavity contains six 10-nm-thick $\text{In}_{0.06}\text{Ga}_{0.94}\text{As}/\text{GaAs}$ quantum wells (QWs). The Rabi splitting is $\Omega=6$ meV. A gradual variation in the active layer thickness along the sample provides a change in the photon mode energy and, hence, in the detuning D between the exciton and photon mode energies at $k=0$. The experiments are carried out in

several regions of the same sample with D in the range from -1.5 to -2 meV.

The sample was placed into an optical cryostat with controlled temperature. A pulsed Ti:sapphire laser with pulse duration of ~ 1 ns, the energy full width at half maximum (FWHM) of ~ 0.7 meV and pulse repetition of 5 kHz, was used for MC excitation at 14° to the cavity normal. The pump beam was focused onto the spot with a waist ~ 100 μm in diameter. The kinetics of the angular distribution of polarized photoluminescence signal from the MC was detected at $T\approx 6$ K in a wide solid angle around the cavity normal by a streak camera with spectral, angular, and time resolution of 0.28 meV, 0.5° , and 70 ps, respectively. The pump transmission signal was detected by the same streak camera.

III. KINETICS OF THE DRIVEN LP MODE

The pump pulse profile $I_{\text{ext}}(t)$ proportional to the intensity of the external electric field outside the cavity $|\mathcal{E}_{\text{ext}}(\mathbf{k}_p, t)|^2$ is shown in Fig. 1(a) (dashed curve). Its intensity increases during the first ~ 100 ps and then decreases approximately three times during ~ 1 ns. MC is excited with pulses polarized linearly in the x direction (their polarization will hereinafter be referred to as π_x polarization), about 0.5 meV above the LP dispersion branch at $\mathbf{k}_p=(k_{p,x}, k_{p,y})=(1.8, 0)$ μm^{-1} . The information on the intracavity field is obtained by MC transmission measurements.³² The active region of the cavity is separated from the detector by a Bragg mirror that does not introduce any nonlinearity and/or spectral selectivity. Hence, the intensity of the pump pulse transmitted through the MC, $I_{\text{tr}}(\omega)$, is proportional to the squared magnitude of the excited mode ($\mathbf{k}=\mathbf{k}_p$) of the intracavity electric field, $|\mathcal{E}_{\text{QW}}(\mathbf{k}_p, \omega)|^2$. Similarly, the time dependences of the transmission intensity $I_{\text{tr}}(t)$ recorded in mutually perpendicular π_x and π_y polarizations are proportional to the corresponding components of the intracavity field intensity, $|\mathcal{E}_{\text{QW},x}(\mathbf{k}_p, t)|^2$ and $|\mathcal{E}_{\text{QW},y}(\mathbf{k}_p, t)|^2$, whereas the time dependence of the first momentum of $I_{\text{tr}}(\hbar\omega)$ provides the information on the temporal evolution of the average energy of the excited LP mode, $\bar{E}_{\text{tr}}(t)$.

Figure 1(a) displays the time dependences of I_{tr} recorded in π_x polarization for several values of peak intensity of the excitation (P) below and above the threshold of stimulated parametric scattering (P_{thr}). P is determined as the maximum of $I_{\text{ext}}(t)$. The transmission signal in π_y polarization is about two orders of magnitude weaker for all excitation densities; it is not shown in Fig. 1. It should be emphasized that conservation of linear polarization is observed only in the case of excitation of the TE or TM modes which correspond to the two-dimensional photon eigenstates in the empty cavity. Excitation of mixture of these modes leads to a strong depolarization of the intracavity field, which is related to the energy splitting of these modes and not discussed in the present paper. At the same time, if the pump is polarized in the TE or TM direction, then the transmission and the scattering signal polarizations do not depend on the actual crystallographic directions. Thus, a crystalline disorder (that, in some cavities,

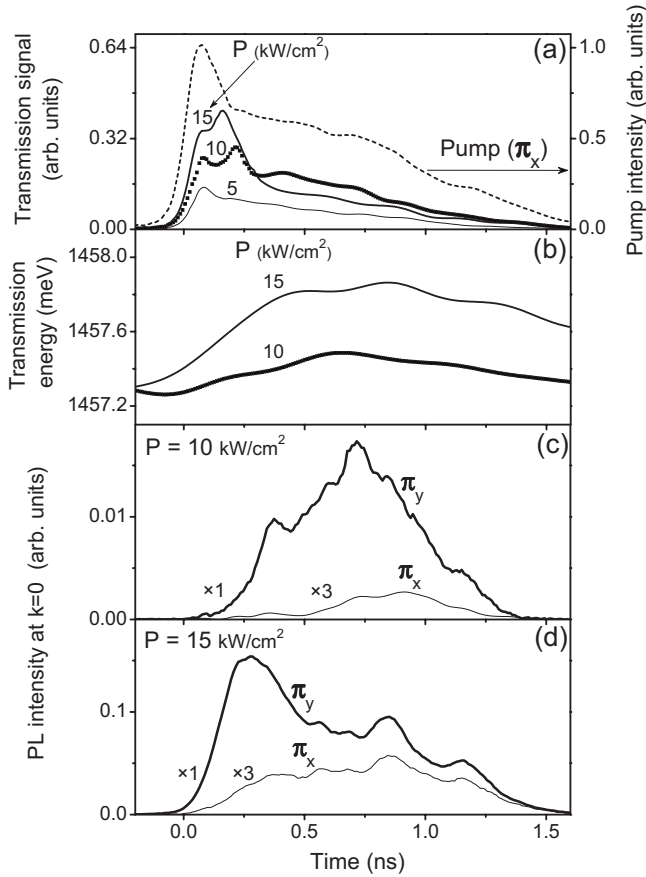


FIG. 1. (a) Time dependences of MC transmission intensity in π_x polarization and (b) spectral position of the transmitted signal for different peak excitation densities (P). Panels (c) and (d) display the emission intensity at $\mathbf{k}=0$ in π_x and π_y polarizations recorded for $P=15$ and 10 kW/cm², respectively. Pump profile is shown in panel (a) by the dashed line labeled as “Pump.” Polarization of the transmission signal coincides with the polarization of the pump (in the case of excitation of the TE or TM polariton modes). Zero time is meant to be approximately corresponding to “switching on” of the pump pulse (the time of reaching the half of the peak pulse intensity).

can result in a large energy splitting of linearly polarized exciton states²⁷) appears to be negligible in our sample.

Figure 1(a) shows that $I_{tr,x}(\mathbf{k}_p, t)$ and, hence, $|\mathcal{E}_{QW,x}(\mathbf{k}_p, t)|^2$ at $P=5$ kW/cm² (obviously below the threshold) are approximately proportional to $I_{ext,x}(t)$. In the range of small P , the spectral position and the FWHM of the transmission signal change very weakly during the pulse propagation, as expected in the linear regime. Strong nonlinearities appear in $I_{tr,x}$ with increase in the peak excitation density above ~ 7 kW/cm². It is seen that $I_{tr,x}$ at $P=10$ kW/cm² exhibits a narrow peak in the range of monotonously decreasing pump density: $I_{tr,x}$ starts increasing at $t \approx 0.1$ ns, increases for about 0.15 ns, and then decreases. With increasing P , the peak shifts slightly toward the pulse onset and increases sharply at $P=15$ kW/cm². The sharp increase in $|\mathcal{E}_{QW,x}(\mathbf{k}_p, t)|^2$ on the droop of exciting pulse occurs due to the instability in the driven LP mode with respect to the incident pump, whereas its subsequent sharp decrease is related to development of the parametric instability with re-

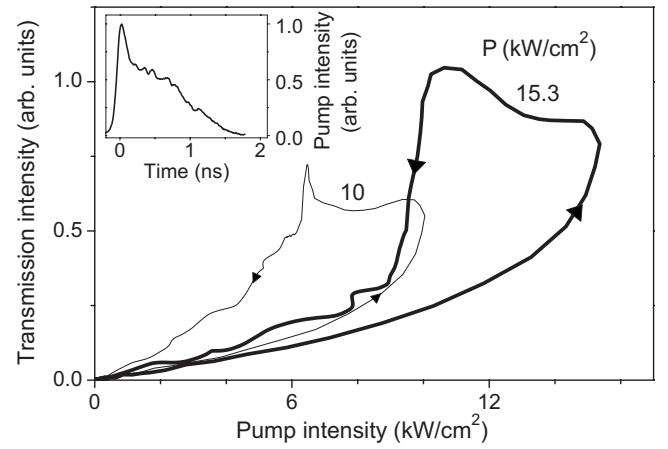


FIG. 2. Measured dependences of transmission intensity I_{tr} on pump intensity I_{ext} for pulses with $P=10$ kW/cm² (thin line) and $P=15.3$ kW/cm² (thick line). Temporal shape of excitation $I_{ext}(t)$ is shown in the inset (it corresponds to the data presented in Fig. 1).

spect to the intermode polariton-polariton scattering^{31,32} that leads to the angular redistribution of the intracavity field.

Entering the range of the instability results in the strong increase in the density of the scattered LPs [Figs. 1(c) and 1(d)]. It is seen in Fig. 1(b) that the blueshift of the driven mode $\Delta\bar{E}(\mathbf{k}_p)$ continues to grow in the range of the decrease in the driven mode magnitude (at 0.2 ns $< t \leq 0.6$ ns). Thus, the contribution of scattered LPs in $\Delta\bar{E}(\mathbf{k}_p)$ overcompensates for the losses caused by the sharp decrease in $\mathcal{E}_{QW}(\mathbf{k}_p, t)$.

The strongly nonequilibrium transitions are legible for the intracavity field drawn as the explicit function of pump intensity. The experimental relationships between $I_{tr,x}(t)$ and $I_{ext,x}(t)$ for $P=10$ and 15.3 kW/cm² presented in the form of $I_{tr,x}(I_{ext,x})$ (equivalent to the dependence of $|\mathcal{E}_{QW,x}(\mathbf{k}_p)|^2$ on $|\mathcal{E}_{ext,x}|^2$) are shown in Fig. 2. $I_{tr,x}$ as a function of $I_{ext,x}$ demonstrates a well pronounced hysteresis behavior and the hysteresis magnitude grows with increasing P . The shape of the hysteresis loop under excitation with linearly polarized light (TE or TM mode) is very similar to that under excitation of the scalar LP system with circularly polarized light. In particular, the temporal delay of the transmission maximum with respect to the excitation peak is explained by the strong positive feedback between the pump and the scattered polariton states that occurs near the threshold of parametric scattering. For instance, the increase in the scattered LP population leads to the blueshift of the exciton energy, which makes the driven LP mode closer to the pump energy even when the pump intensity decreases. As a result, the sharp nonequilibrium transformation accompanied by the rapid increase in the overall polariton density can occur on the descending side of the pulse (see Ref. 32 for the detailed consideration). In a vicinity close to the threshold, the system is very sensitive to fluctuations in both the pump and the intracavity field, and the kinetics of the system strongly depends on the certain temporal shape of the excitation pulse.

On the other hand, as soon as the blow-up transition has already occurred, additional fluctuations have no appreciable influence on the state of the system. In the high-intensity state, the effective resonance energy of the driven mode ex-

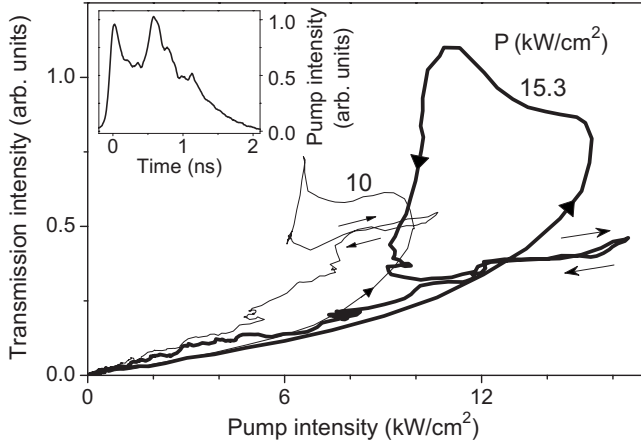


FIG. 3. Measured dependences of transmission intensity I_{tr} on pump intensity I_{ext} for double-peaked pulses with $P=10$ kW/cm² (thin line) and $P=15.3$ kW/cm² (thick line). Temporal shape of the excitation $I_{ext}(t)$ is shown in the inset.

ceeds the pump energy due to the blueshift provided in part by the scattered LP population. In that region, the response function is smooth; it corresponds to the upper branch of the “S”-shaped figure which represents the function of the stationary response of a typical bistable system. Thus, the changes induced by additional fluctuations should be reversible. To verify that the system was tested by means of excitation pulse with an additional maximum at $t \approx 0.6$ ns (Fig. 3). The experimental relationships between $I_{tr,x}(t)$ and $I_{ext,x}(t)$ in the case of excitation with two-peaked pulses at $P=10$ and 15.3 kW/cm² are drawn in the form of $I_{tr,x}(I_{ext,x})$. It is seen that, as expected, no additional hysteresis loops appear in the range of the second peak of excitation, in contrast to the preceding nonequilibrium transformation that induces the prominent hysteresis. In the range of the second peak, the intensity of the driven mode ($I_{tr}(t) \propto |\mathcal{E}_{QW}(\mathbf{k}_p, t)|^2$) is much smaller than the maximum of $I_{tr}(t)$ (reached during the “blow-up” transition), although the energy of transmission $[\bar{E}_{tr}(t)]$ at $t \approx 0.7$ ns is the largest even in the case of single-peaked excitation [Fig. 1(b)]. It means that the driven mode is kept near resonance with the pump due to the blueshift provided by the scattered polaritons.

In summary, the LP system excited with linearly polarized light exhibits a hysteresis behavior qualitatively similar to the case of circular excitation. One of the aims of the present work is to study the influence of the polarization-dependent properties of the LP-LP interactions on the system behavior, in view of the predictions made in the framework of the preceding theoretical consideration. Let us mention its most essential ideas and a possible way of their experimental validation. Generally, the physical nature of the hysteresis in the system response to excitation consists in an effective dependence of the LP resonance energy on the intracavity field amplitude. The blueshift resulting from the exciton-exciton repulsive interaction leads to the bistability of the stationary response in the case when the pump energy exceeds the energy of the unperturbed LP state. Bistability implies the presence of intrinsic critical states of the driven mode, even in the absence of the intermode scattering. For the driven mode

itself, small fluctuations of pump intensity near the critical magnitude (P_{crit}) may cause a sharp increase in the intracavity field. The critical pump intensity depends on polariton interaction strength which, in turn, is essentially spin dependent (in particular, the interaction between polaritons with opposite spins is attractive,³⁴ which is indirectly confirmed by the polarization inversion in the process of parametric scattering, see Refs. 26 and 27 and Sec. IV below). Henceforth the critical points for the driven polariton mode should strongly depend on pump polarization, which results in an essentially multistable response of the driven mode under the action of cw pump.³⁷ For instance, the critical pump magnitude for linearly polarized excitation should be approximately two times larger than that for a circular one (because of the two times smaller blueshift in the former case). On the other hand, polarization of the intracavity field may be strongly dependent on variations in pump intensity (assuming that the polarization of the pump is kept invariable). According to the predictions in Ref. 37, even when the pump is polarized linearly, the intracavity field may acquire a large circular polarization in a certain range of the pump intensities.

In contrast to the above-mentioned prediction, we observed no signs of polarization multistability of the intracavity field induced by linearly polarized excitation. In particular, polarization of the MC transmission retains the polarization of pump in the whole range of pump densities. Thus, it is of interest to compare the kinetics of the critical transformation of the driven LP mode for the cases of circular and linear polarizations of excitation.

Figure 4 compares the shapes of MC transmittance I_{tr}/I_{ext} for excitations with σ - and π -polarized light at peak excitation densities close to the critical value (P_{crit}). In both cases the MC transmittance at $P=5.2$ kW/cm² reaches its maximum in the range of the pulse maximum and then decreases; the response functions are approximately reversible. Such behavior corresponds to the smooth change in the blueshift of the driven mode. In contrast, the response functions for both cases of σ - and π -polarized light at $P=7.2$ kW/cm² exhibit an evident hysteresis behavior with very similar hysteresis loops. It means that the critical pump densities appear to be almost coincident for these polarizations. Thus, the experiment does not show any increase in P_{crit} for excitation with π -polarized light.

The visible absence of the difference in P_{crit} for π - and σ -polarized excitations agrees with the absence of multistability in the response of the driven LP mode. However, these results raise the question why the decreased repulsion in the linearly polarized LP system does not lead to the corresponding increase in P_{crit} . Among possible reasons, one can consider several effects neglected in the model in Ref. 37, e.g., incoherent LP scattering (assisted by phonons, free carriers, etc.), an increase in the LP-LP scattering of π -polarized LPs due to the proximity of $2\hbar\omega_{pump}$ to the biexciton resonance,³⁸ the saturation effects (at high exciton densities) which result in the additional blueshift of LPs due to the decrease in the exciton-photon coupling constant, etc. Additional experiments are required to determine which of the mentioned phenomena plays the dominant role.

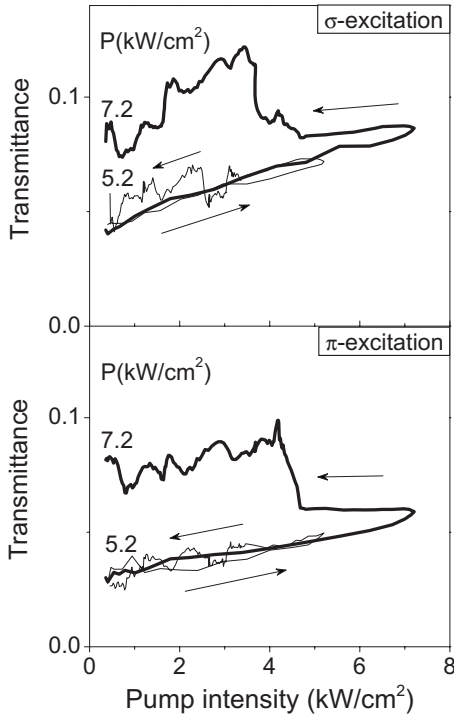


FIG. 4. Measured dependences of MC transmittance I_{tr}/I_{ext} on pump intensity I_{ext} for the cases of circular and linear polarizations of pump (upper and lower panels, respectively). Thin and thick lines correspond to peak pump densities $P=5.2$ and 7.2 kW/cm^2 , respectively.

IV. KINETICS OF SIGNAL OF STIMULATED POLARITON SCATTERING

The time dependences of the emission signal at $\mathbf{k}=0$ in two linear polarizations (π_x and π_y) are displayed in Figs. 1(c) and 1(d) for the two peak excitation densities above P_{thr} . The exciting pulse has the π_x polarization. It is seen that, in contrast to the electric field in the driven mode $\mathbf{k}=\mathbf{k}_p$, the signal at $\mathbf{k}=0$ does not retain the polarization of excitation. The emission in the π_y polarization (i) appears earlier and (ii) exceeds markedly that in the π_x polarization. Measurements of the signal components in circular σ^\pm polarizations (not presented in Fig. 1) showed that they coincide with each other, which points to the absence of ellipticity in the signal polarization. Such behavior shows that the kinetics of the scattering signal at $\mathbf{k}=0$ is strongly influenced by the polarization dependence of the LP-LP interactions. The inversion of the signal polarization observed in our pulse measurements is in good agreement with the previous observations of this effect in cw measurements.^{26,27}

The kinetics of the signal at $\mathbf{k}_p=0$ in the dominating π_y polarization, $I_{s,y}(t)$, is very similar to that under the excitation with circularly polarized light (see Ref. 31). Indeed, Fig. 1 shows that (i) the dependences $I_{s,y}(t)$ differ qualitatively from both the exciting field $I_{ext}(t)$ and the intracavity field $|\mathcal{E}_{QW}(\mathbf{k}_p, t)|^2 \propto I_{tr}(t)$, (ii) $I_{s,y}(t)$ grows exponentially in the range of the sharp decrease in $|\mathcal{E}_{QW}(\mathbf{k}_p, t)|^2$, and (iii) the maximum of $I_{s,y}$ shifts monotonously to the onset of the exciting pulse with increasing P (according to the shift of the parametrically unstable range of pump intensities).

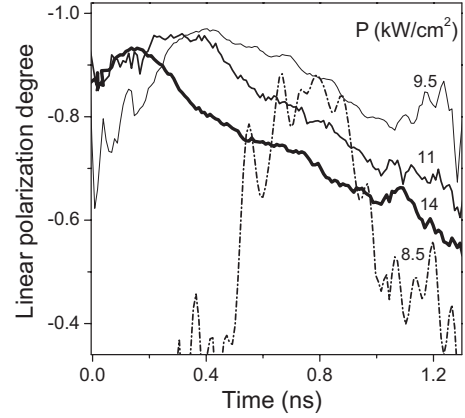


FIG. 5. (a) Time dependences of linear polarization degree of the scattering signal, $\rho_{s,lin}=(I_{s,x}-I_{s,y})/(I_{s,x}+I_{s,y})$, for various peak excitation densities ($P \geq P_{thr}$). The pump is polarized in the x direction. The corresponding degree of circular polarization does not exceed 10% in the above-threshold area.

Figures 1(c) and 1(d) show that the signal in π_x polarization is very small at the beginning of the stimulated scattering process but its relative intensity increases monotonously with time. Time dependences of the degree of linear polarization $\rho_{s,lin}=(I_{s,x}-I_{s,y})/(I_{s,x}+I_{s,y})$ at $P \geq P_{thr}$ are displayed in Fig. 5. $|\rho_{s,lin}|$ at $P \sim P_{thr} \approx 8.5$ kW/cm^2 is less than 0.5 at the beginning of the pulse ($t < 0.4$ ns), increases quickly up to the value 0.8 ± 0.1 with increasing signal intensity, exceeds 0.8 in the range of the signal maximum, and then decreases quickly at $t > 1$ ns simultaneously with the signal decay. With increase in the peak pump intensity, the maximum of $|\rho_{s,lin}|$ shifts to the beginning of the pump pulse, which correlates with the earlier development of the parametric instability and reaches 0.93 ± 0.03 . Finally, Fig. 5 shows that $|\rho_{s,lin}|$ decreases slightly with time after the formation of the stimulated scattering signal.

High polarization of the signal is well expected for the process of direct scattering $(\mathbf{k}_p, \mathbf{k}_p) \rightarrow (\mathbf{k}, 2\mathbf{k}_p - \mathbf{k})$ accompanied by inversion of linear polarization.²⁶ This process provides the main contribution to the signal intensity. On the other hand, the polarization of the signal evidently decreases with time (whereas the polarization of the driven mode remains constant), which indicates a relative decrease in the contribution of the mentioned direct scattering. The reasons for that are not sufficiently clear. The increase in $I_{s,x}$ at $\mathbf{k}=0$ may be due to the “secondary” scattering processes which involve π_y -polarized LPs with $\mathbf{k} \neq 0$. It should be emphasized that the observed decrease in linear polarization is not accompanied by appearance of ellipticity, which is characteristic of an arbitrary mixture of different polarization components. Note, however, that the measured polarization is the result of averaging over 10^5 independent excitation pulses. In this connection, the observed depolarization of the emission signal may be caused by the averaging that dilutes the correlations between the phases of the σ^\pm components of the intracavity field.

The dependences of the time-integrated signal intensities on peak pump intensity in two linear polarizations are shown in Fig. 6. In both polarizations, the signal demonstrates a

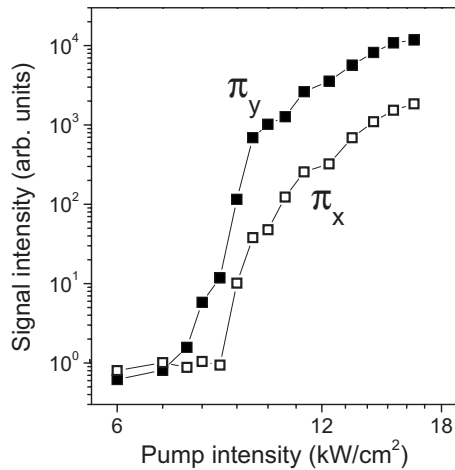


FIG. 6. Dependences of the integral signal intensities in two linear polarizations on pump intensity for π_x -polarized excitation. The corresponding σ^\pm -polarized components are equal for all pump intensities.

thresholdlike growth with increasing P , however, the threshold densities do not coincide: the threshold for π_x polarization is larger by approximately 20%. Below the threshold of parametric scattering, the signal polarization is very weak. With increasing peak pump intensity, the strongly dominating π_y polarization of the signal appears due to the “direct” LP-LP scattering (breakup of the driven polariton state). The polarization degree of the time-integrated signal exceeds 0.9 at $P=1.2P_{\text{thr}}$ and then decreases with further increase in the pump intensity. Eventually, the fraction of the π_x -polarized component of the field at $\mathbf{k}=0$ reaches 15% at $P > 1.5P_{\text{thr}}$.

V. CONCLUSION

We have investigated the polarization-dependent kinetics of the MC polariton system excited with linearly polarized nanosecond-long pump pulses. Intensities and polarizations

have been measured for both the driven and the $\mathbf{k}=0$ signal polariton modes. It has allowed the direct tracing the polariton spin dynamics near the threshold of parametric instability.

The driven mode is found to retain the linear polarization of the incident pulse; thus, no manifestations of polarization multistability discussed in Ref. 37 are observed. With increasing pump intensity, the driven mode demonstrates parametric instabilities similar to those in the scalar LP system excited with circularly polarized light. The development of the instabilities results in the stimulated polariton-polariton scattering. The polarization of the scattering signal is perpendicular to that of the incident pump, which points to an attraction between excitons with opposite spins. Significant depolarization of the scattering signal during the pulse propagation is observed only at excitation densities well above the threshold (P_{thr}).

The experimental results are discussed within the framework of the mean-field model based on the Gross-Pitaevskii equations which takes into account the only mechanism of shift of exciton eigenenergy, namely, blueshift or redshift caused by the direct pairwise polariton-polariton interactions.^{26,34,37} Within this model, one expects a strong dependence of the threshold pump density on pump polarization.³⁷ In contrast, we found no noticeable change in the critical pump intensities when the pump polarization was switched from circular to linear one. This result points to factors that are beyond the scope of the conventional model; they should be clarified by further research of the polarization-dependent properties of polariton systems.

ACKNOWLEDGMENTS

We are grateful to N. A. Gippius and S. G. Tikhodev for valuable remarks and fruitful discussions, M. S. Skolnick for rendered samples, and A. V. Larionov for assistance in the experiment. This work was supported by the Russian Foundation for Basic Research and the Russian Academy of Sciences.

¹G. Khitrova, H. M. Gibbs, F. Jahnke, M. Kira, and S. W. Koch, *Rev. Mod. Phys.* **71**, 1591 (1999).

²M. S. Skolnick, A. I. Tartakovskii, R. Butte, D. M. Whittaker, and R. M. Stevenson, *IEEE J. Sel. Top. Quantum Electron.* **8**, 1060 (2002).

³A. Kavokin and G. Malpuech, *Cavity Polaritons* (Elsevier/North-Holland, Amsterdam, 2003).

⁴P. G. Savvidis, J. J. Baumberg, R. M. Stevenson, M. S. Skolnick, D. M. Whittaker, and J. S. Roberts, *Phys. Rev. Lett.* **84**, 1547 (2000).

⁵A. I. Tartakovskii, D. N. Krizhanovskii, and V. D. Kulakovskii, *Phys. Rev. B* **62**, R13298 (2000).

⁶R. M. Stevenson, V. N. Astratov, M. S. Skolnick, D. M. Whittaker, M. Emam-Ismael, A. I. Tartakovskii, P. G. Savvidis, J. J. Baumberg, and J. S. Roberts, *Phys. Rev. Lett.* **85**, 3680 (2000).

⁷J. J. Baumberg, P. G. Savvidis, R. M. Stevenson, A. I. Tartakovskii, M. S. Skolnick, D. M. Whittaker, and J. S. Roberts, *Phys. Rev. B* **62**, R16247 (2000).

⁸V. D. Kulakovskii, A. I. Tartakovskii, D. N. Krizhanovskii, N. A. Gippius, M. S. Skolnick, and J. S. Roberts, *Nanotechnology* **12**, 475 (2001).

⁹R. Butte, M. S. Skolnick, D. M. Whittaker, D. Bajoni, and J. S. Roberts, *Phys. Rev. B* **68**, 115325 (2003).

¹⁰H. Deng, G. Weihs, C. Santori, J. Bloch, and Y. Yamamoto, *Science* **298**, 199 (2002).

¹¹M. Richard, J. Kasprzak, R. Andre, R. Romestain, Le Si Dang, G. Malpuech, and A. Kavokin, *Phys. Rev. B* **72**, 201301(R) (2005).

¹²J. Kasprzak, M. Richard, S. Kundermann, A. Baas, P. Jeambrun, J. M. J. Keeling, F. M. Marchetti, M. H. Szymanska, R. Andre, J. L. Staehli, V. Savona, P. B. Littlewood, B. Deveaud, and Le Si Dang, *Nature (London)* **443**, 409 (2006).

- ¹³R. Balili, V. Hartwell, D. Snoko, L. Pfeiffer, and K. West, *Science* **316**, 1007 (2007).
- ¹⁴A. Baas, J.-Ph. Karr, M. Romanelli, A. Bramati, and E. Giacobino, *Phys. Rev. B* **70**, 161307(R) (2004).
- ¹⁵D. M. Whittaker, *Phys. Rev. B* **71**, 115301 (2005).
- ¹⁶N. A. Gippius, S. G. Tikhodeev, V. D. Kulakovskii, D. N. Krizhanovskii, and A. I. Tartakovskii, *Europhys. Lett.* **67**, 997 (2004).
- ¹⁷N. A. Gippius and S. G. Tikhodeev, *J. Phys.: Condens. Matter* **16**, S3653 (2004).
- ¹⁸C. Ciuti and I. Carusotto, *Phys. Status Solidi B* **242**, 2224 (2005).
- ¹⁹S. S. Gavrilov, N. A. Gippius, V. D. Kulakovskii, and S. G. Tikhodeev, *Sov. Phys. JETP* **104**, 715 (2007).
- ²⁰M. Wouters and I. Carusotto, *Phys. Rev. B* **75**, 075332 (2007).
- ²¹C. Ciuti, P. Schwendimann, and A. Quattropani, *Phys. Rev. B* **63**, 041303(R) (2001).
- ²²D. M. Whittaker, *Phys. Rev. B* **63**, 193305 (2001).
- ²³W. Langbein, *Phys. Rev. B* **70**, 205301 (2004).
- ²⁴G. Panzarini, L. C. Andreani, A. Armitage, D. Baxter, M. S. Skolnick, V. N. Astratov, J. S. Roberts, A. V. Kavokin, M. R. Vladimirova, and M. A. Kaliteevski, *Phys. Rev. B* **59**, 5082 (1999).
- ²⁵A. Kavokin, P. G. Lagoudakis, G. Malpuech, and J. J. Baumberg, *Phys. Rev. B* **67**, 195321 (2003).
- ²⁶K. V. Kavokin, P. Renucci, T. Amand, X. Marie, P. Senellart, J. Bloch, and B. Sermage, *Phys. Status Solidi C* **2**, 763 (2005).
- ²⁷D. N. Krizhanovskii, D. Sanvitto, I. A. Shelykh, M. M. Glazov, G. Malpuech, D. D. Solnyshkov, A. Kavokin, S. Ceccarelli, M. S. Skolnick, and J. S. Roberts, *Phys. Rev. B* **73**, 073303 (2006).
- ²⁸I. A. Shelykh, Y. G. Rubo, G. Malpuech, D. D. Solnyshkov, and A. Kavokin, *Phys. Rev. Lett.* **97**, 066402 (2006).
- ²⁹A. I. Tartakovskii, D. N. Krizhanovskii, D. A. Kurysh, V. D. Kulakovskii, M. S. Skolnick, and J. S. Roberts, *Phys. Rev. B* **65**, 081308(R) (2002).
- ³⁰P. G. Lagoudakis, P. G. Savvidis, J. J. Baumberg, D. M. Whittaker, P. R. Eastham, M. S. Skolnick, and J. S. Roberts, *Phys. Rev. B* **65**, 161310(R) (2002).
- ³¹A. A. Demenev, A. A. Shchekin, A. V. Larionov, S. S. Gavrilov, V. D. Kulakovskii, N. A. Gippius, and S. G. Tikhodeev, *Phys. Rev. Lett.* **101**, 136401 (2008).
- ³²A. A. Demenev, A. A. Shchekin, A. V. Larionov, S. S. Gavrilov, and V. D. Kulakovskii, *Phys. Rev. B* **79**, 165308 (2009).
- ³³J. I. Inoue, T. Brandes, and A. Shimizu, *Phys. Rev. B* **61**, 2863 (2000).
- ³⁴P. Renucci, T. Amand, X. Marie, P. Senellart, J. Bloch, B. Sermage, and K. V. Kavokin, *Phys. Rev. B* **72**, 075317 (2005).
- ³⁵Y. Yamamoto, F. Tassone, and H. Cao, *Semiconductor Cavity Quantum Electrodynamics*, Springer Tracts in Modern Physics Vol. 169 (Springer-Verlag, Heidelberg, 2000).
- ³⁶C. Ciuti, V. Savona, C. Piermarocchi, A. Quattropani, and P. Schwendimann, *Phys. Rev. B* **58**, 7926 (1998).
- ³⁷N. A. Gippius, I. A. Shelykh, D. D. Solnyshkov, S. S. Gavrilov, Yuri G. Rubo, A. V. Kavokin, S. G. Tikhodeev, and G. Malpuech, *Phys. Rev. Lett.* **98**, 236401 (2007).
- ³⁸M. Wouters, *Phys. Rev. B* **76**, 045319 (2007).